Journal of Metals, Materials and Minerals, 36(1), e2406, 2026

Effect of garnet incorporation on the functional properties of sunscreens

Parinya CHAKARTNARODOM[1], Kanyarat MUNMANI[1], Sureerat POLSILAPA[1], Duangrudee CHAYSUWAN[1], Wichit PRAKAYPAN[2], Passakorn SONPRASARN[3], Edward A. LAITILA[4], and Nuntaporn KONGKAJUN[5,6,*]

[1] *Department of Materials Engineering, Faculty of Engineering, Kasetsart University, Bangkok, 10900, Thailand*
[2] *Source Runner Enterprise Co. Ltd., Bangkok, 10220, Thailand*
[3] *Sun Cement Process Co. Ltd., Ratchaburi, 70120, Thailand*
[4] *Department of Materials Science and Engineering, Michigan Technological University, Houghton, MI, 49931, USA*
[5] *Department of Materials and Textile Technology, Faculty of Science and Technology, Thammasat University, Pathumthani,12121, Thailand*
[6] *Thammasat University Research Unit in Sustainable Materials and Circular Economy, Thammasat University, Pathumthani,12121, Thailand*

***Corresponding author e-mail**: n-kongkj@tu.ac.th

Received date:
17 May 2025
Revised date:
21 August 2025
Accepted date:
5 November 2025

Keywords:
Garnet;
Sunscreen;
UV;
SPF;
Water resistance

Abstract

Garnet, a silicate mineral, was investigated as a replacement for the TiO_2-based compound in sunscreen formulations. Samples containing garnet were evaluated for color shade, viscosity, sun protection factor (SPF), and water resistance. Substituting the TiO_2-based compound with garnet reduced both viscosity and SPF but markedly enhanced water resistance. This improvement is attributed to the physical reinforcement provided by garnet particles, which strengthen the sunscreen film and reduce wash-off under water exposure. Garnet incorporation also altered the product's appearance from white to a darker brownish-beige tone, improving visual compatibility with a wider range of skin tones.

1. Introduction

Exposure to the sun offers benefits for humans, including the production of vitamin D3 in the form of cholecalciferol [1]. However, excessive exposure can lead to various skin problems such as cracks, burns, immune suppression, wrinkles, dermatitis, urticaria, premature aging, hypopigmentation, hyperpigmentation, and an increased risk of cancer. Ultraviolet (UV) protection can be achieved through physical measures by wearing protective clothing, sunglasses, hats, and using an umbrella. Additionally, sunscreen is a commonly used form of protection, as it can absorb or reflect UV radiation. A typical sunscreen contains inorganic ingredients such as a mixture of titanium dioxide (TiO_2), kaolin, talc, zinc oxide (ZnO), calcium carbonate ($CaCO_3$), and magnesium oxide (MgO) [2].

Although sunscreen is highly effective for UV protection, especially at the beach, its chemical components have harmful effects on marine life. Studies have shown that certain chemicals in sunscreen can impair the early developmental stages of sea urchins [3] and cause damage to coral reefs [4]. According to the U.S. National Ocean Service [5], harmful chemicals that can negatively impact marine ecosystems include oxybenzone, benzophenone-1, benzophenone-8, OD-PABA, 4-methylbenzylidene camphor, 3-benzylidene camphor, nano-titanium dioxide, nano-zinc oxide, octinoxate, and octocrylene.

Garnet is a silicate mineral commonly found in metamorphic and igneous rocks, such as gneisses and schists, as well as in garnet-rich sands formed by the erosion of these rocks. While typically red, garnet can also be found in a range of colors, including colorless, black, brown, yellow, and green. Its general chemical formula is $A_3B_2Si_3O_{12}$, where A represents calcium, magnesium, iron, manganese, or a combination of these elements, and B represents aluminum, iron, vanadium, zirconium, titanium, or chromium, or a combination of these elements. The main garnet-producing countries are India, China, Australia, and the United States. Garnet is primarily used as an abrasive and a gemstone in jewelry; being employed in various industries for applications such as water jet cutting, abrasive blasting media and powder, as well as for filtering grains, and general abrasives grit. [6-10].

With environmental sustainability gaining increasing importance in the construction materials industry, garnet is being researched as a potential fine aggregate and supplementary cementitious material [8,11-13]. A study by Kunchariyakun and Sukmak [14] highlights an additional advantage of incorporating garnet into cement mortar: it enhances radiation shielding properties, improving gamma-ray and neutron shielding by 34% and 26%, respectively, compared to the control sample. Garnet's radiation shielding benefits suggests incorporation into sunscreens could elevate performance, various

mixtures of added garnet will be evaluated by focusing on sun protection factor (SPF), viscosity, and water resistance.

2. Experimental

2.1 Sunscreen production

The raw materials used in sunscreen production are classified into three groups (A, B, and C) based on their functions, as detailed in Table 1. Titanium dioxide (TiO_2) and zinc oxide (ZnO) are commonly used UV filters, with TiO_2 being more effective in the UVB range (290 nm to 320 nm) and ZnO in the UVA range (320 nm to 400 nm) [15].

The various sunscreen formulations used in this study are presented in Table 2. The reference formulation (Formula Ref), a standard sunscreen base, served as the control. According to the U.S. Food and Drug Administration (FDA) [16], erythema, or sunburn, is primarily induced by UVB exposure. To evaluate the potential of garnet in mitigating erythema, it was incorporated as a replacement for the TiO_2-based compound in formulations SC1 through SC7. In addition to UV protection, cosmetic elegance is an important attribute of sunscreen, defined by its invisibility on the skin and smooth spreadability, similar to lotions or foundations [17]. However, formulations containing metal oxides such as TiO_2 often produce a white cast upon application, which reduces user acceptability [17]. To address this limitation, the present work explores the use of garnet as a substitute for TiO_2, leveraging its inherent coloration to minimize whitening while maintaining protective performance.

The garnet was sourced from a flotation plant in Tak, Thailand, and the TiO_2-based compound was a cosmetic-grade product obtained from a commercial supplier of raw materials for cosmetic manufacturing. The phase compositions of the garnet and the TiO_2–based compound were analyzed using an X-ray diffractometer (XRD, PANalytical Empyrean), while their chemical compositions were determined with an X-ray fluorescence spectrometer (XRF, Bruker S2 PUMA Series II). Additionally, the wetting characteristics of these materials are determined using a contact angle meter (Kyowa DM-CE1), and their UV absorption capabilities were assessed with a UV–visible diffuse reflectance spectrophotometer (UV-Vis DRS, Shimadzu ISR-2600Plus).

To produce the sunscreen, the materials in groups A and B (Table 1) were first mixed separately in beakers using a glass stirring rod. The group A materials were then transferred to a homogenizer (Figure 1(a)) and mixed at 1000 rpm for 10 min. Next, the group B materials were gradually added while increasing the mixing speed to 1500 rpm. Finally, the group C material was incorporated and mixed for an additional minute.

Before mixing with other materials, the garnet was ground using a planetary ball mill (Fritsch Pulverisette 6, Figure 1(b)) operated at 580 rpm with alumina balls. The alumina balls had an average diameter of 12.33 mm and a total weight of 117.91 g. The grinding process took 18 min for 100 g of garnet. It was then sieved through mesh sizes No. 200, 325, and 400. Only the garnet particles that passed through the 400 mesh sieve were used in sunscreen production. Figure 1(c-e) illustrates the garnet at three stages: before grinding, after grinding, and after passing through a 400 mesh sieve. Additionally, the TiO_2–based compound used is shown in Figure 1(f) in its powder form.

Table 1. Raw materials used in sunscreen production and their functions.

Group	No.	Chemical	Function
A	1	Garnet powder	UV Filter
	2	TiO_2–based compound	UV Filter
	3	ZnO	UV Filter
	4	Hydrogenated dimer dilinoleyl	Emollient, Texture enhancer
	5	Dibutyl adipate	Emollient, Solubilizer
	6	Cocoglycerides	Emollient, Solubilizer
	7	C12-15 alkyl benzoate	Emollient, Solubilizer, Water-resistant agent
	8	Polyglyceryl-2 triisostearate	O/W emulsifier
	9	Cetyl PEG/PPG-10/1 dimethicone	Silicone emulsifier
B	10	Water	Solvent
	11	Disodium EDTA	Chelating agent
	12	Propylene glycol	Humectant, solvent
C	13	Phenoxyethanol 97%, Capryly l g	Preservative

Table 1. Formulations used for sunscreen production.

No.	Chemical	Formula [wt%]							
		Ref	SC1	SC2	SC3	SC4	SC5	SC6	SC7
1	Garnet powder	0	1	2	3	6	10	14	20
2	TiO_2–based compound	20	19	18	17	14	10	6	0
3	Zinc oxide (ZnO)	5	5	5	5	5	5	5	5
4	Hydrogenated dimer dilinoleyl	5	5	5	5	5	5	5	5
5	Dibutyl adipate	5	5	5	5	5	5	5	5
6	Cocoglycerides	5	5	5	5	5	5	5	5
7	C12-15 alkyl benzoate	10	10	10	10	10	10	10	10
8	Polyglyceryl-2 triisostearate	3	3	3	3	3	3	3	3
9	Cetyl PEG/PPG-10/1 dimethicone	1.5	1.5	1.5	1.5	1.5	1.5	1.5	1.5
10	Water	41.6	41.6	41.6	41.6	41.6	41.6	41.6	41.6
11	Disodium EDTA	0.2	0.2	0.2	0.2	0.2	0.2	0.2	0.2
12	Propylene glycol	3	3	3	3	3	3	3	3
13	Phenoxyethanol 97%, Caprylyl g	0.7	0.7	0.7	0.7	0.7	0.7	0.7	0.7

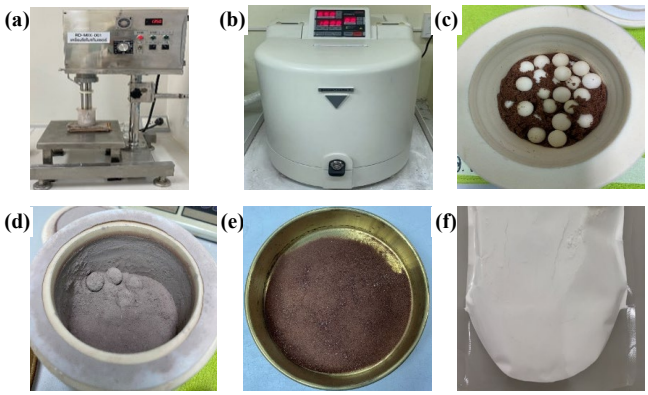

Figure 1. Instruments and raw materials used in this study: (a) Homogenizer machine, (b) high-speed ball milling machine, (c) garnet before milling, (d) garnet after milling, (e) garnet passed through a 400 mesh sieve, and (f) TiO_2-based compound in powder form, contained in a plastic package.

Figure 2. Viscometer.

The morphology of the finely ground garnet was imaged using a scanning electron microscope (SEM, Hitachi SU3500) equipped with an energy-dispersive spectrometer (EDS). Additionally, the particle size of both the finely ground garnet and TiO_2–based compound used in this study were measured with a laser particle size distribution analyzer (Mastersizer 3000).

2.2 Physical characteristics of sunscreens

The appearance of the sunscreen samples is visually assessed. Their viscosity was measured using a rotational viscometer (Brookfield DV2T) equipped with an RV spindle, operated at 1.5 rpm on a 200 g sample for 30 s to 60 s or until a stable reading was obtained, as shown in Figure 2.

2.3 Sunscreen effectiveness

The effectiveness of sunscreen is evaluated based on its SPF and water resistance. The SPF quantifies the sunscreen's ability to protect the skin from erythema caused by UV radiation exposure [18]. This was measured using an in vitro test following the ISO 23675 standard [19]. The sunscreen was applied to a polymethyl methacrylate (PMMA) substrate according to the procedure outlined in the ISO 24443 standard [20]. The PMMA substrate had a minimum area of 0.5 cm^2, with approximately 1.3 $mg \cdot cm^{-2}$ of sunscreen applied. After application, the coated substrate was left in a dark area for 30 min before being analyzed using an ultraviolet transmittance analyzer (Labsphere UV-2000S) to determine SPF, following Equation (1).

$$\text{In vitro SPF} = \frac{\int_{290\,nm}^{400\,nm} E(\lambda)I(\lambda)d\lambda}{\int_{290nm}^{400nm} E(\lambda)I(\lambda)T(\lambda)d\lambda} \quad (1)$$

Varible $E(\lambda)$ represents the erythema action spectrum, $I(\lambda)$ is the spectral irradiance of the UV source, and $T(\lambda)$ denotes the spectral transmittance of the sample [21,22]. The wavelength range from 290 nm to 400 nm covers both UVA and UVB regions [15]. Each substrate was measured nine times to determine the average in vitro SPF value, with three substrates tested for each sunscreen formula.

According to the U.S. FDA [16], the water resistance of a sunscreen indicates how well its labeled SPF protection is maintained after immersion in water for a specified period. In other words, water resistance refers to the ability of a sunscreen to maintain its effectiveness during activities involving water exposure, such as swimming, or after sweating for a certain period of time [23]. The water resistance of the sunscreen was evaluated following the procedure outlined in the ISO 16217 standard [24]. The measurement process was as follows. After the in vitro SPF measurement, as described in the previous paragraph, the substrate was immersed in 5 mL of deionized water at 30°C, with the pH adjusted to 6.5 to 7.5 and a conductivity of at least 500 µS. The water was stirred using a fan rotating at 100 rpm for 20 min. The substrate was then allowed to air dry. This procedure was repeated one more time before conducting a final in vitro SPF measurement.

The water resistance of a sunscreen is calculated using Equation (2), where %WRR denotes the percentage water resistance retention, and SPFs and SPFw represent the SPF of the sunscreen before and after the water resistance testing, respectively [25].

$$\%WRR = \frac{(SPF_w - 1)}{(SPF_s - 1)} \times 100 \quad (2)$$

3. Results and discussion

3.1 Chemical composition and particle size analysis of garnet and the TiO_2–based compound

The XRF results for both the garnet and the TiO_2–based compound are presented in Table 3. The primary oxides identified in the garnet are Al_2O_3, SiO_2, MnO, and Fe_2O_3. In contrast, the TiO_2–based compound consists mainly of TiO_2, along with other oxides such as Al_2O_3, SiO_2, Fe_2O_3, MgO, and K_2O.

The XRD pattern of garnet (Figure 3(a)) reveals Mn^{2+}-bearing almandine (PDF card no. 00-033-0658) as the primary phase, with the chemical formula $(Fe,Mn)_3Al_2(SiO_4)_3$. For the TiO_2-based compound (Figure 3(b)), the dominant phase is rutile TiO_2 (PDF card no. 01-079-6029), accompanied by a secondary fluorophlogopite mica phase (PDF card no. 01-082-2904) with the chemical formula $K_{0.91}(Fe_{0.61}Mg_{2.39})(Al_{0.92}Si_{3.08})O_{10}(O_{0.74}F_{1.26})$. As noted by Fontán *et al.* [26] and Kim *et al.* [27], mica is commonly incorporated into cosmetic formulations to impart a shimmering effect while also enhancing protection against harmful solar radiation.

Table 2. Chemical compositions of garnet and TiO_2–based compound.

Material	Oxide [wt %]							
	Al_2O_3	SiO_2	MnO	Fe_2O_3	TiO_2	MgO	K_2O	Others
Garnet	17.88	34.75	19.45	27.92				
TiO_2–based compound	6.19	12.37		0.03	74.38	4.96	1.88	0.19

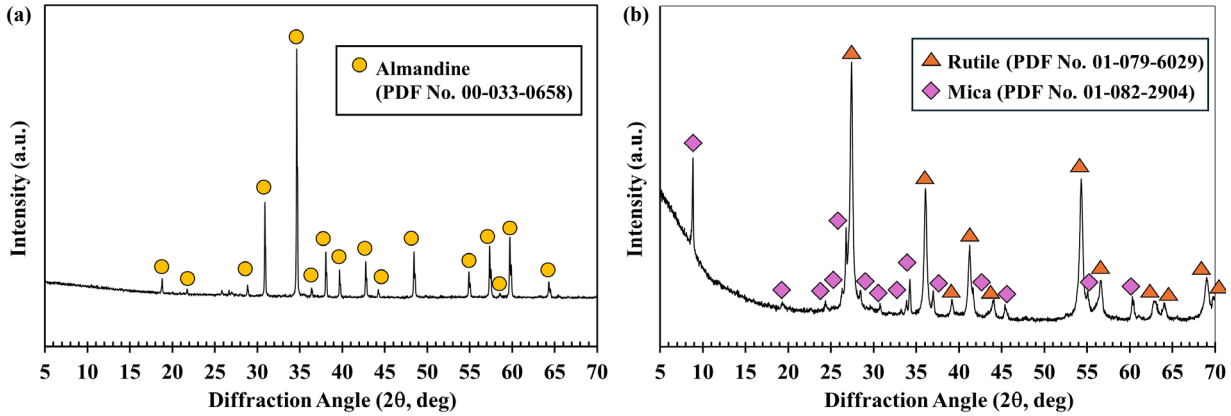

Figure 3. XRD patterns of (a) garnet and (b) TiO_2–based compound.

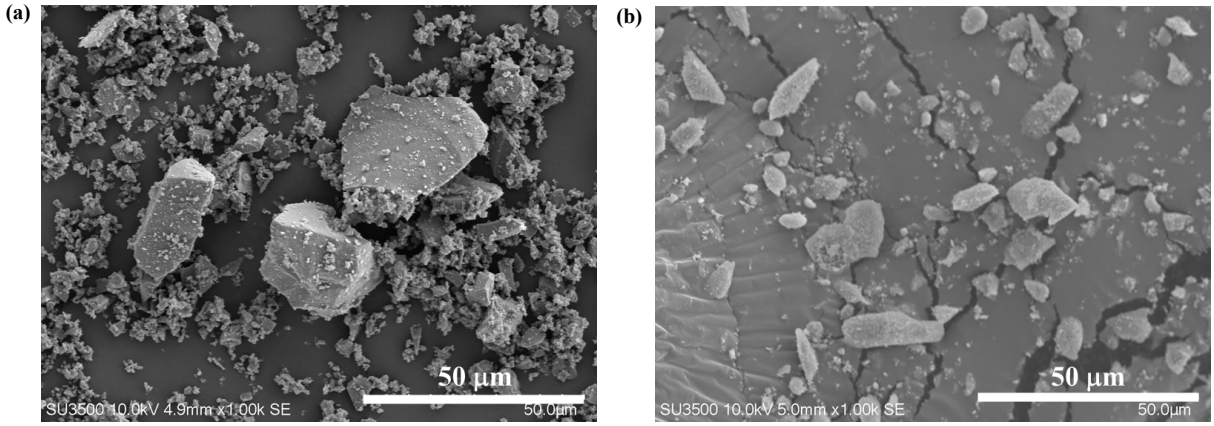

Figure 4. SEM images of (a) garnet particles and (b) TiO_2-based compound particles.

Figure 4(a) shows garnet particles with a wide size distribution, where the larger particles appear angular and relatively smooth. The TiO_2-based compound in Figure 4(b) also exhibits broad size variation, consisting of fine particles along with larger agglomerates. Figure 5 and Figure 6 present the EDS mappings of garnet and the TiO_2-based compound, respectively, highlighting their elemental distributions. In garnet (Figure 5), Al, Si, Mn, Fe, and O are detected, while the TiO_2-based compound (Figure 6) contains Ti, Mg, Al, Si, K, Fe, and O. These findings are consistent with the XRF results. Particle size distribution analysis (Figure 7) further reveals that the median particle size of garnet is 7.43 µm ± 0.04 µm, compared to 5.47 µm ± 0.01 µm for the TiO_2-based compound.

3.2 Properties of the sunscreens

The various color shades of the sunscreen samples are presented in Figure 6. The sunscreen from the reference formula (Ref) appears white, which may result in a visible white cast on many skin tones. Formula SC1 exhibits a light beige tone, while SC2 and SC3 show slightly warmer beige tones. Sunscreens from formulas SC4, SC5, and SC6 display progressively darker, more neutral, or grayish beige tones. In formula SC7, where the TiO_2–based compound is entirely replaced with garnet, the sunscreen shows a deeper brown or slightly reddish-brown shade.

Based on these appearances, the Ref formula may not be suitable for most skin tones due to its whiteness. Formulas SC1, SC2, and SC3 may be better matched with light skin tones, while SC4, SC5, and SC6 may be suitable for medium to tan skin tones. For darker skin tones, formula SC7 may offer the best match.

According to Chang *et al.* [28], the color change of an object can be evaluated using its RGB values. With recent advances in computer software, these values can be accurately extracted from digital images [29]. In this study, the color shade of each sample in Figure 8 was determined using the Eyedropper tool in Microsoft PowerPoint (Microsoft 365). The obtained RGB values were then converted to CIE Lab coordinates using Colormine [30], an online tool for color value conversion referenced in [29].

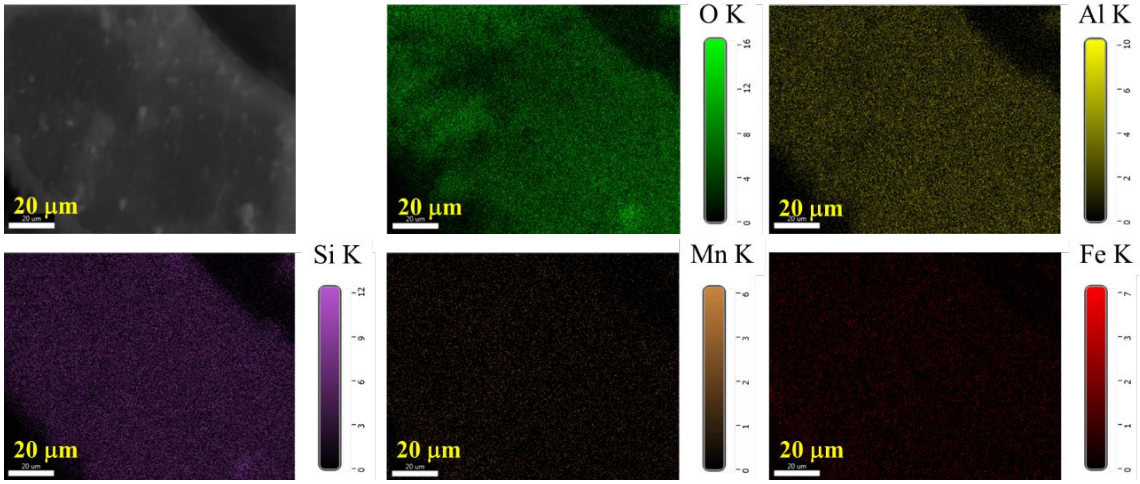

Figure 5. EDS mapping showing the elemental distribution in garnet.

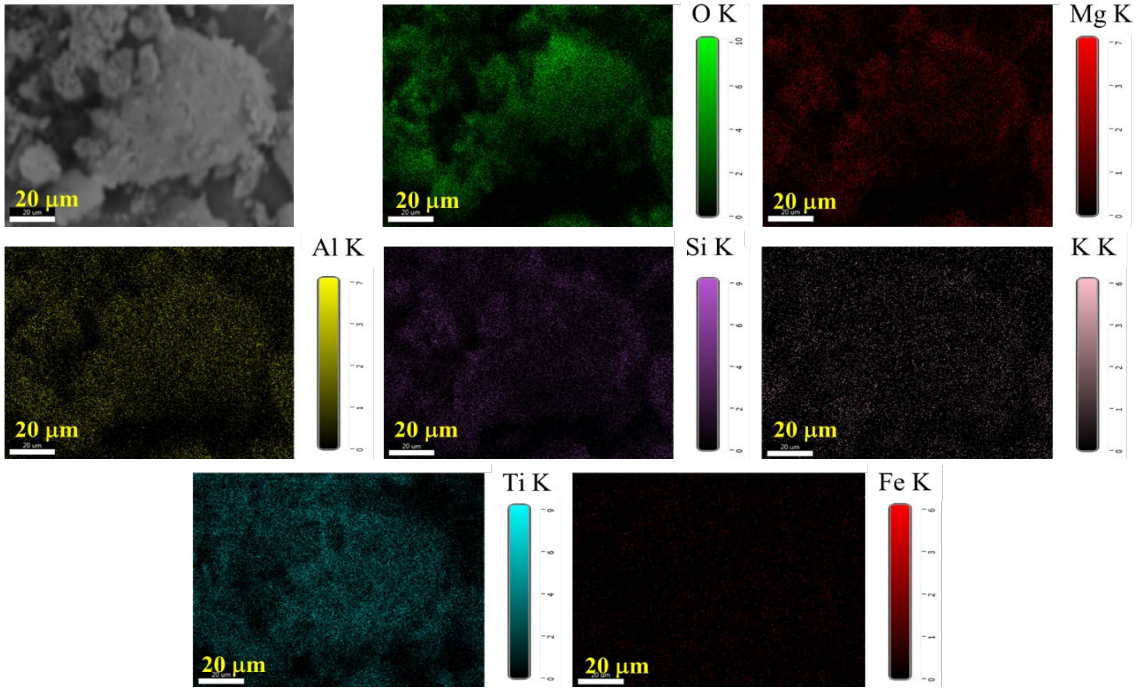

Figure 6. EDS mapping showing the elemental distribution in TiO_2-based compound**.**

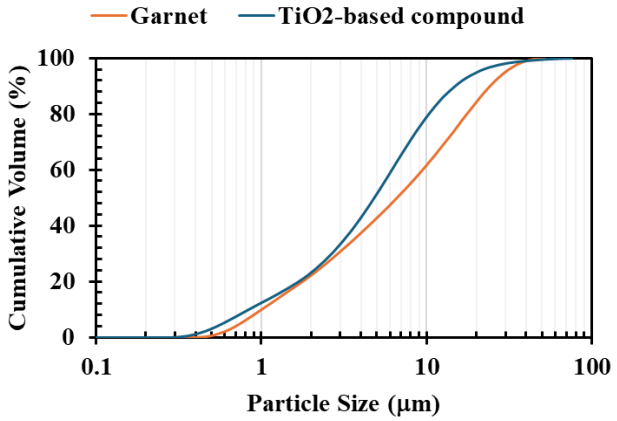

Figure 7. Particle size distribution of garnet and the TiO_2–based compound.

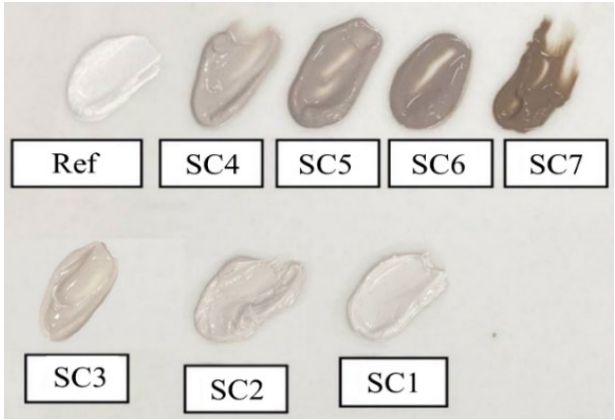

Figure 8. Appearance of sunscreen samples.

Table 3. Color measurements of the sunscreen samples.

Sample	RGB values			CIE Lab coordinates		
	R	G	B	L*	a*	b*
Ref	233	230	225	91.39	0.140	2.778
SC1	221	218	209	87.05	-0.549	4.775
SC2	218	211	201	84.85	0.681	5.791
SC3	212	197	190	80.54	4.061	5.387
SC4	193	183	174	74.99	1.973	5.829
SC5	172	158	149	66.05	3.552	6.538
SC6	151	134	127	57.23	5.206	6.106
SC7	129	110	96	47.83	5.129	10.57

For shade comparison, the RGB values were converted to grayscale values (Y) using the following Equation [3]:

$$Y = 0.2989R + 0.5870G + 0.1140B \quad (3)$$

In addition, color comparison was performed based on the color difference (ΔE) between the sunscreen samples and the reference formula, calculated from the CIE Lab coordinates as follows [29]:

$$\Delta E = \sqrt{\Delta L^2 + \Delta a^2 + \Delta b^2} \quad (4)$$

where ΔL, Δa, and Δb represent the differences in the L*, a*, and b* values of the sunscreen samples relative to the reference formula.

The RGB values and CIE Lab coordinates of the sunscreen samples are presented in Table 4. Their corresponding grayscale values, calculated using Equation (3), are shown in Figure 9, while the ΔE values, calculated using Equation (4), are shown in Figure 10. Grayscale values typically range from 0 (black) to 255 (white) [32], with lower values indicating darker shades. As shown in Figure 9, the grayscale values decrease linearly as the TiO_2-based compound is progressively replaced with garnet, demonstrating that garnet incorporation darkens the sunscreen. Furthermore, Figure 10 shows that ΔE values increase with higher garnet content, confirming that the addition of garnet significantly alters the sunscreen color. This results in a darker shade that is more compatible with various skin tones and may help eliminate the white cast commonly associated with TiO_2 in commercial sunscreens.

The viscosity of the sunscreen samples decreases linearly as the TiO_2-based compound is progressively replaced with garnet (Figure 11), enhancing spreadability on the skin. As previously noted, the median particle size of garnet is larger than that of the TiO_2-based compound. Arai *et al.* [33] stated that liquids containing smaller dispersed particles generally exhibit higher viscosity than those with larger particles at the same volume fraction. Similarly, Wang *et al.* [34] demonstrated that smaller particle sizes (with larger surface area) promote stronger surface charge interactions, which increase resistance to fluid flow and result in higher viscosity. Therefore, the incorporation of garnet increases the average particle size of the mixture, weakens interparticle interactions, and consequently reduces viscosity, as shown in Figure 11.

According to the World Health Organization (WHO) [35], sunscreen must have an SPF of at least 30 to provide effective protection against skin cancer. The *in vitro* SPF values of sunscreen samples are shown in Figure 12. Obviously, replacing the TiO_2–based compound with garnet leads to a reduction in SPF, only formulas Ref, SC1, SC2, and SC3 meet the minimum SPF requirement. Furthermore, based on the trendline, the maximum amount of garnet that can replace the TiO_2–based compound while still maintaining adequate SPF protection is approximately 21%.

The garnet is less effective than the TiO_2–based compound in absorbing UV radiation within the UVB range (290 nm to 320 nm), Figure 13. Consequently, partially replacing the TiO_2–based compound with garnet leads to a reduction in the sunscreen's SPF, as observed in Figure 12.

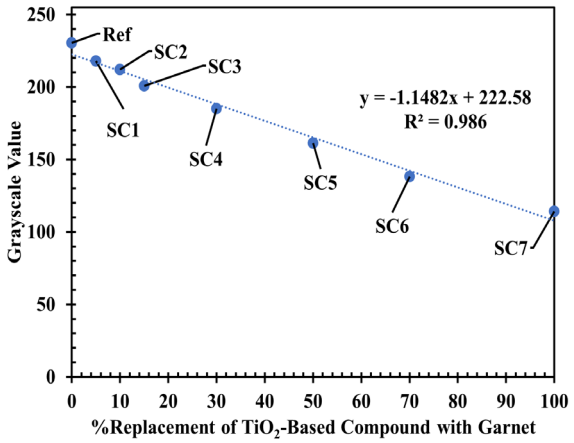

Figure 9. Grayscale values of the sunscreen samples.

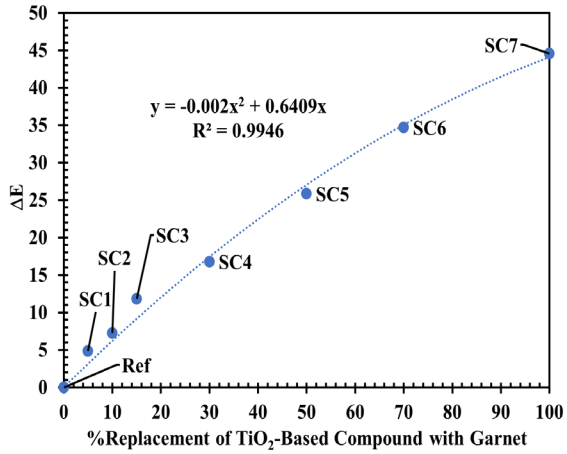

Figure 10. Color difference (ΔE) of the sunscreen samples compared with the reference formula.

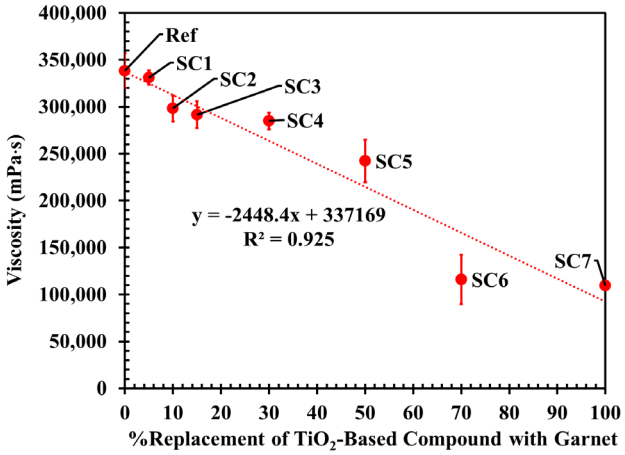

Figure 11. Viscosity of the sunscreen samples.

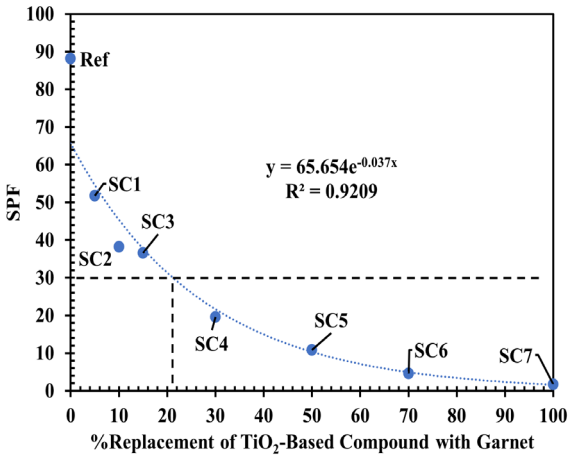

Figure 12. In vitro SPF of the sunscreen samples.

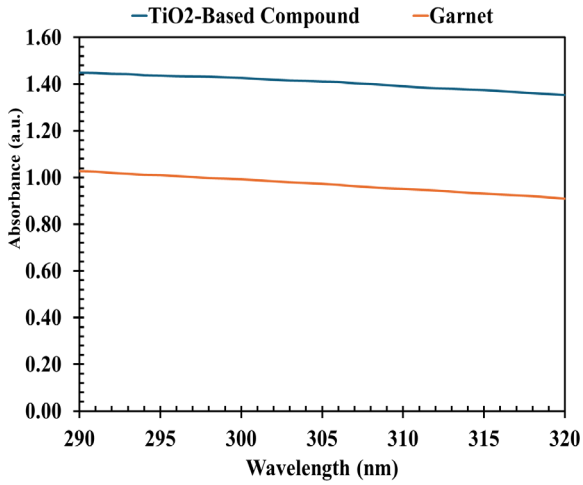

Figure 13. Absorption of TiO_2–based compound and garnet in the UVB range (290 nm to 320 nm).

For sunscreens containing metal oxide UV filters, the primary mechanism of UV protection is absorption [17]. In the case of rutile TiO_2, its band gap of approximately 3.03 eV [36] enables it to absorb photons with energies above this threshold, corresponding to wavelengths shorter than about 409 nm. This property allows rutile TiO_2 to exhibit strong absorption across the UV region [17]. Similarly, Kou *et al.* [37] reported that fluorophlogopite mica has a band gap of 3.96 eV, which also lies within the UV range.

In contrast, absorption in garnet arises from the presence of transition metal elements such as Mn and Fe within its crystal structure. Zhu and Guo [38] reported that Mn^{2+} produces characteristic absorption peaks at approximately 408 nm, 460 nm, and 480 nm due to electronic d–d transitions. Additionally, Izawa *et al.* [39] demonstrated that Fe^{2+} exhibits absorption at wavelengths above 430 nm. Therefore, compared to garnet, TiO_2-based compound is more effective in absorbing UV radiation across the relevant region.

The water resistance retention of sunscreens with initial SPF values above 30—including formulas Ref, SC1, SC2, and SC3—is presented in Figure 14. According to Couteau *et al.* [40], a sunscreen is considered water resistant if its retention exceeds 50%. All tested formulas met this criterion, with SC1, SC2, and SC3 demonstrating superior water resistance compared to the Ref formula.

As highlighted by Keshavarzi *et al.* [41], sunscreen water resistance can be enhanced either by increasing hydrophobicity to repel water or by improving adhesion to the outermost skin layer. To assess this, garnet and the TiO_2-based compound were compacted into small discs for contact angle measurement. The results showed that garnet is hydrophilic, while the TiO_2-based compound is hydrophobic (Figure 15). Thus, the improved water resistance observed in SC1, SC2, and SC3 cannot be explained by increased hydrophobicity alone.

Hydrophilicity refers to a material's ability to attract and interact with water, typically evaluated through contact angle measurements, with lower angles indicating stronger hydrophilicity [42]. Garnet and TiO_2 are both intrinsically hydrophilic due to surface hydroxyl groups that readily interact with water [43-47]. In contrast, Kou *et al.* [37] reported that fluorophlogopite mica is hydrophobic, which accounts for the hydrophobic character of the TiO_2-based compound.

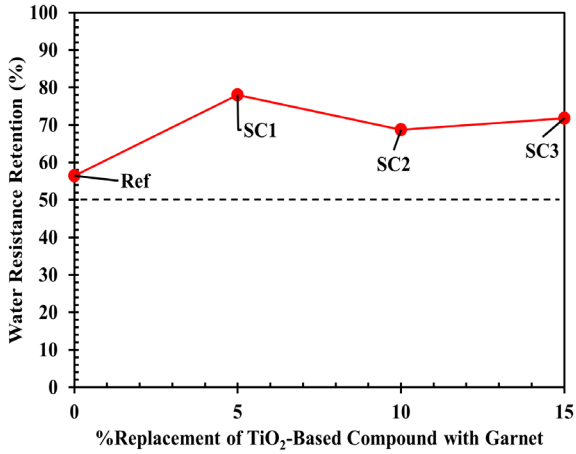

Figure 14. Water resistance retention of the sunscreen samples.

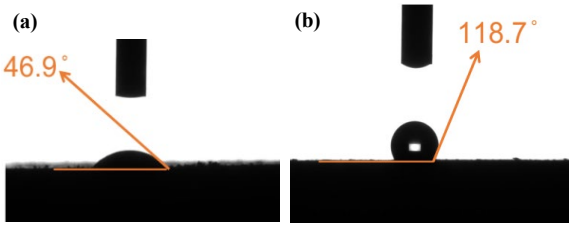

Figure 15. Wetting characteristics of (a) garnet, and (b) TiO_2-based compound.

The enhanced water resistance of the garnet-containing sunscreens is therefore likely attributed to a physical mechanism. Jiang *et al.* [48] investigated natural garnet–reinforced epoxy matrix composites and found that the incorporation of garnet improved the hardness, resistance to decomposition, and wear resistance of the composites. Similarly, in this study, garnet particles are believed to reinforce the structural integrity of the protective film formed on the substrate, creating a more durable and resilient barrier. Unlike chemical repellency, this mechanical reinforcement minimizes film degradation and wash-off when exposed to water or sweat, thereby enhancing the overall water resistance of the sunscreen.

4. Conclusions

The performance of garnet-incorporated sunscreens was assessed, revealing several key effects. Garnet addition gradually shifted the product color from white to a dark brownish beige, improving compatibility across diverse skin tones. Substituting the TiO_2-based compound with garnet reduced both viscosity and SPF, but significantly enhanced water resistance. This enhancement is attributed to the physical reinforcement provided by garnet particles, which strengthen the sunscreen film and minimize wash-off during water exposure.

Declaration of competing interest

The authors declare that they have no known competing financial interests or personal relationships that could have appeared to influence the work reported in this article.

Data availability

Data will be made available on request.

Acknowledgement

This work was funded by the Faculty of Engineering, Kasetsart University [Grant Number 65/08/MAT/Innovation]. We gratefully acknowledge the Department of Materials Engineering, Faculty of Engineering, Kasetsart University, and Cosmania Laboratories Co., Ltd. for their instrumental support. Special thanks are extended to Cosmania Laboratories Co., Ltd. and Glass Bridge Co., Ltd. for providing materials used in this study. We also sincerely thank the technical staff of both the Department of Materials Engineering and Cosmania Laboratories Co., Ltd. for their valuable assistance.

References

[1] R. Nasution, R. Azura, M. Bahi, N. B. Maulydia, R. A. Bastian, M. M. Hilda, and M. Marianne, "In silico investigation of γ-Sitosterol isolated from the ethanol extract of artocarpus camansi leaves as a sunscreen agent," *Indonesian Journal of Chemistry,* Article vol. 25, no. 1, pp. 221-231, 2025.

[2] D. M. Manikrao, and D. S. Laxman, "Sunscreens: A review," *Pharmacognosy Journals,* vol. 8, no. 3, 2016.

[3] C. Corinaldesi, E. Damiani, F. Marcellini, C. Falugi, L. Tiano, F. Bruge, and R. Danovaro, "Sunscreen products impair the early developmental stages of the sea urchin Paracentrotus lividus," *Scientific Reports,* vol. 7, no. 1, p. 7815, 2017.

[4] D. Olson, "The Truth About Corals and Sunscreen." [Online]. Available: https://ocean.si.edu/ecosystems/coral-reefs/truth-about-corals-and-sunscreen.

[5] US National Ocean Service, "Skincare chemicals and coral reefs." [Online]. Available: https://oceanservice.noaa.gov/news/sunscreen-corals.html.

[6] R.V. Dietrich, "Garnet," in *Britannica*, ed, 2025.

[7] D. C. Stewart, "Garnet (mineral)," in *Salem Press Encyclopedia of Science*, ed, 2023.

[8] N. F. A. Jamaludin, K. Muthusamy, N. N. Isa, M. F. Md Jaafar, and N. Ghazali, "Use of spent garnet in industry: A review," *Materials Today: Proceedings,* vol. 48, pp. 728-733, 2022.

[9] C. Balasubramaniyan, K. Rajkumar, B. Suresh Krishnan, and A. Arun, "Performance evaluation of abrasive water jet machining on spent garnet reinforced hybrid composite," *Materials Today: Proceedings,* vol. 98, pp. 16-20, 2024.

[10] G.-W. Joo, T.-M. Oh, H.-J. Hwang, and G.-C. Cho, "Evaluating the efficacy of recycled garnet abrasives in enhancing hard rock cutting performance of abrasive waterjet systems," *International Journal of Rock Mechanics and Mining Sciences,* vol. 167, p. 105407, 2023..

[11] N. F. A. Jamaludin, K. Muthusamy, M. F. Md Jaafar, Z. Ali, Z. Abdul Majid, and M. A. Ismail, "Preliminary investigation on spent garnet as a novel supplementary cementitious material," *Construction and Building Materials,* vol. 451, p. 138789, 2024.

[12] K. R. Usman, M. R. Hainin, M. K. Idham, M. Satar, M. N. M. Warid, A. Usman, Z. H. Al-Saffar, and M. A. Bilema, "A comparative assessment of the physical and microstructural properties of waste garnet generated from automated and manual blasting process," *Case Studies in Construction Materials,* vol. 14, p. e00474, 2021.

[13] H. L. Muttashar, N. B. Ali, M. A. Mohd Ariffin, and M. W. Hussin, "Microstructures and physical properties of waste garnets as a promising construction materials," *Case Studies in Construction Materials,* vol. 8, pp. 87-96, 2018.

[14] K. Kunchariyakun, and P. Sukmak, "Utilization of garnet residue in radiation shielding cement mortar," *Construction and Building Materials,* vol. 262, p. 120122, 2020.

[15] T. Smijs, and S. Pavel, "Titanium dioxide and zinc oxide nanoparticles in sunscreens: Focus on their safety and effectiveness," *Nanotechnol Sci Appl,* vol. 4, pp. 95–112, 2011.

[16] US Food and Drug Administration, "Guidance for industry labeling and effectiveness testing: sunscreen drug products for overthe-counter human use — small entity compliance guide." [Online]. Available: https://www.fda.gov/media/85172/ download

[17] A. J. Addae and P. S. Weiss, "Standardizing the white cast potential of sunscreens with metal oxide ultraviolet filters," *Accounts of Materials Research,* vol. 5, no. 4, pp. 392-399, 2024.

[18] K. Geoffrey, A. N. Mwangi, and S. M. Maru, "Sunscreen products: Rationale for use, formulation development and regulatory considerations," *Saudi Pharmaceutical Journal*, vol. 27, no. 7, pp. 1009-1018, 2019.

[19] ISO 23675: 2021 Cosmetics — Sun protection test methods — In Vitro determination of Sun Protection Factor (SPF),

International Organization for Standardization, Switzerland, 2021.

[20] *ISO 24443:2021 Cosmetics — Determination of sunscreen UVA photoprotection in vitro*, International Organization for Standardization, Switzerland, 2021.

[21] A. Springsteen, R. Yurek, M. Frazier, and K. F. Carr, "In vitro measurement of sun protection factor of sunscreens by diffuse transmittance," *Analytica Chimica Acta,* vol. 380, no. 2, pp. 155-164, 1999.

[22] J. F. Dlugos, "A Spectroscopic In vitro method for the calculation of sunscreen spf values." [Online]. Available: https://resources.perkinelmer.com/lab-solutions/resources/docs/APP_Spectroscopic-InVitro-Sunscreen-SPF-Values.pdf

[23] W. Zou, R. Ramanathan, S. Urban, C. Sinclair, K. King, R. Tinker, and V. Bansal, "Sunscreen testing: A critical perspective and future roadmap," *TrAC Trends in Analytical Chemistry,* vol. 157, p. 116724, 2022.

[24] *ISO 16217:2020 Cosmetics — Sun protection test methods — Water immersion procedure for determining water resistance*, International Organization for Standardization, Switzerland, 2020.

[25] M. Pissavini, V. Alard, U. Heinrich, K. Jenni, V. Perier, V. Tournier, D. Lutz, M. Meloni, D. Kockott, L. Ferrero, B. Gonzalez, L. Zastrow, and H. Tronnier, "In vitro assessment of water resistance of sun care products: A reproducible and optimized in vitro test method," *International journal of cosmetic science,* vol. 29, pp. 451-460, 2008.

[26] M. Rincón-Fontán, L. Rodríguez-López, X. Vecino, J. M. Cruz, and A. B. Moldes, "Design and characterization of greener sunscreen formulations based on mica powder and a biosurfactant extract," *Powder Technology,* vol. 327, pp. 442-448, 2018.

[27] J. Kim, J. Choi, S. Choi, W. Kim, and S. Lee, "Study on the dependence of sun protection factor on particle size distribution of mica using gravitational field-flow fractionation: Dependence of SPF on particle size distribution of mica," *Bulletin of the Korean Chemical Society,* vol. 41, 2019.

[28] Y.-H. Chang, P.-H. Huang, B.-Y. Wu, and S.-W. Chang, "A study on the color change benefits of sustainable green building materials," *Construction and Building Materials,* vol. 83, pp. 1-6, 2015.

[29] M. Xaba, S. Mapukata, and T. Mokhena, "ChatGPT based method for obtaining repeatable and quantitative colorimetric measurements," *MethodsX,* vol. 15, p. 103525, 2025.

[30] Colormine. https://colormine.org/convert/rgb-to-lab (accessed 2025).

[31] M. Ullah, J. Mir, and A. Ahmad, "Assessing the influence of cement replacement materials on concrete performance through image processing," *Measurement,* vol. 256, p. 118014, 2025.

[32] L. Tan, and J. Jiang, "Chapter 13 - Image processing basics," in *Digital Signal Processing (Third Edition)*, L. Tan, and J. Jiang Eds.: Academic Press, 2019, pp. 649-726.

[33] Y. Arai, T. Tomai, G. Seong, R. Ito, A. Yoko, and T. Adschiri, "Unified formulation of particle-size-dependent viscosity for Newtonian dispersions of micro- and nanoparticles," *Journal of Molecular Liquids,* vol. 411, p. 125659, 2024.

[34] C. Wang, J. Zhang, and L. Lei, "Effect of particle size on silicon nitride ceramic slurry by stereolithography," *Journal of Wuhan University of Technology- Materials Science Edition,* vol. 38, no. 3, pp. 514-519, 2023.

[35] World Health Organization (WHO). "Radiation: Protecting against skin cancer." https://www.who.int/news-room/questions-and-answers/item/radiation-protecting-against-skin-cancer (accessed 2025).

[36] Y. Etafa Tasisa, T. Kumar Sarma, R. Krishnaraj, and S. Sarma, "Band gap engineering of titanium dioxide (TiO_2) nanoparticles prepared via green route and its visible light driven for environmental remediation," *Results in Chemistry,* vol. 11, p. 101850, 2024..

[37] Y. Kou, D. Liao, T. Du, L. Peng, and Y. Wang, "Zincophilic-hydrophobic fluorophlogopite mica protective layer enables dendrite-free and anticorrosive Zn anodes," *Chemical Engineering Journal,* vol. 508, p. 160888, 2025.

[38] M. Zhu, and Y. Guo, "Combined colorimetry and spectroscopy: A novel nondestructive method for identifying orange garnet species," *Spectrochimica Acta Part A: Molecular and Biomolecular Spectroscopy,* vol. 341, p. 126461, 2025.

[39] M. R. M. Izawa, E. A. Cloutis, T. Rhind, S. A. Mertzman, J. Poitras, D. M. Applin, and P. Mann, "Spectral reflectance (0.35–2.5 μm) properties of garnets: Implications for remote sensing detection and characterization," *Icarus,* vol. 300, pp. 392-410, 2018.

[40] C. Couteau, D. Alexandre, C. Clotilde, and L. J. M. and Coiffard, "Influence of the hydrophilic–lipophilic balance of sunscreen emulsions on their water resistance property," *Drug Development and Industrial Pharmacy,* vol. 38, no. 11, pp. 1405-1407, 2012.

[41] F. Keshavarzi, N. Knudsen, N. M. Komjani, M. F. Ebbesen, J. Brewer, S. Jafarzadeh, and E. Thormann, "Enhancing the sweat resistance of sunscreens," *Skin Research and Technology,* vol. 28, no. 2, pp. 225-235, 2022.

[42] I. Fenoglio, B. Fubini, E. M. Ghibaudi, and F. Turci, "Multiple aspects of the interaction of biomacromolecules with inorganic surfaces," *Advanced Drug Delivery Reviews,* vol. 63, no. 13, pp. 1186-1209, 2011.

[43] Z. Zhang, C. Fan, F. Jiao, and Q. Wei, "Garnet in the flotation of fine-grained lepidolite: Strengthening role and action mechanism," *Colloids and Surfaces A: Physicochemical and Engineering Aspects,* vol. 716, p. 136730, 2025.

[44] J. Poon, D. C. Madden, M. H. Wood, R. van Tol, H. Sonke, and S. M. Clarke, "Surface chemistry of almandine garnet," *The Journal of Physical Chemistry C,* vol. 124, no. 9, pp. 5099-5117, 2020.

[45] Y. Xi, Y. Qi, Z. Mao, Z. Yang, and J. Zhang, "Surface hydrophobic modification of TiO_2 and its application to preparing PMMA/TiO_2 composite cool material with improved hydrophobicity and anti-icing property," *Construction and Building Materials,* vol. 266, p. 120916, 2021.

[46] N. Sakai, A. Fujishima, T. Watanabe, and K. Hashimoto, "Quantitative evaluation of the photoinduced hydrophilic conversion properties of TiO_2 thin film surfaces by the reciprocal of contact angle," *The Journal of Physical Chemistry B,* vol. 107, no. 4, pp. 1028-1035, 2003.

[47] C.-Y. Wu, K.-J. Tu, J.-P. Deng, Y.-S. Lo, and C.-H. Wu,

"Markedly enhanced surface hydroxyl groups of TiO_2 nanoparticles with superior water-dispersibility for photocatalysis," *Materials*, vol. 10, no. 5, p. 566, 2017.

[48] Y. Jiang, F. Xu, K. Liu, and Q. Feng, "Surface-modified garnet particles for reinforcing epoxy composites," *Minerals*, vol. 8, no. 5, p. 217, 2018.